ACTA PHYSICA DEBRECINA XLVI, 57 (2012)

GUIDING OF 3 KEV AR^{7+} IONS BY POLYCARBONATE NANOCAPILLARIES AND GLASS MICROCAPILLARIES

P. Herczku[1], Z. Juhász[1], S.T.S. Kovács[2], S. Biri[1], R. P. Rácz[1] and B. Sulik[1]

[1] Institute of Nuclear Research (Atomki), Bem tér 18/c, H-4026 Debrecen, Hungary
[2] University of Debrecen, Egyetem tér 1, H-4032 Debrecen, Hungary

Abstract

In the present work dynamic properties of the guiding of 3 keV Ar^{7+} ions by polycarbonate (PC) and glass capillaries at 5° tilt angle are studied together with that of the transmitted neutrals. The guided ions and the outgoing neutrals were separated by an electrostatic field in front of a position sensitive multichannel plate detector system. For the PC sample, after a maximum guided transmission, we observed a strong blocking effect. The glass sample exhibited a very slow development for the guided transmission of both ions and neutrals. This is in contrast to earlier results for ion guiding by a single glass capillary.

I. Introduction

The phenomenon of ion guiding through tilted insulating nanocapillaries is a topic of increasing interest [1-6]. The guiding effect is due to the deposited charges on the inner capillary walls which are able to deflect the highly charged ions towards the exit, along the capillary axis [1]. In this work we present the result of two experiments performed for studying how the guiding effect develops in time. In the experiments 3 keV Ar^{7+} ions

were sent through capillary arrays of different sizes and materials. A comparisons was made between results for polycabonate samples, which were presented in also ref. [8], and new results for glass capillary arrays.

II. Experimental method

Both experiments were performed at the Electron Cyclotron Resonance Ion Source (ECRIS) of Atomki. The extracted Ar^{7+} ion beam of 3 keV energy was collimated to a diameter of 0.5 mm before entering the experimental chamber. The base pressure of the chamber was about $6{\cdot}10^{-7}$ mbar. The schematic view of the experimental arrangement can be seen in figure 1. Our sample holder is movable in three independent directions, and it is rotatable around the z axis, for setting the tilt angle of the sample, Ψ (see Fig. 1). We used a position sensitive multichannel plate detector (MCP) system for measuring the transmitted ions and neutralized Ar atoms. The detector can be rotated around the same axis as the sample holder. This way we can ensure that the guided particles always arrive to the central region of detector. In front of the MCP detector we used a pair of electrostatic deflector plates in order to separate the different charge states. The typical voltage applied on it was 1 kV.

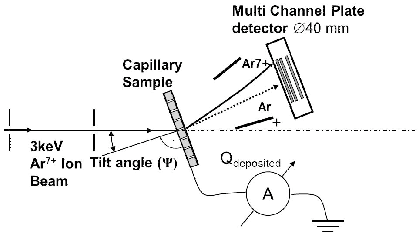

Figure 1: Schematic view of the experimental arrangement.

In the first experiment, we investigated the dynamic properties of the guiding effect for 3 keV Ar^{7+} ions by nanocapillaries created in polycarbonate (PC) foil. We used a commercially available filter-foil sample, in which the capillaries were prepared by swift heavy ion irradiation followed by alkaline etching of the ion tracks. The diameter of the capillaries was

about 170 nm, and their length was 30 μm. The geometric opening was estimated to 9.5 percent from scanning electron microscopy (SEM) pictures. For foils with random capillary distribution (which are produced by ion-irradiation) this is considered to be a high capillary density. For avoiding macroscopic charge-up effects, the surface of the sample was covered with a thin ($\sim$20 nm) gold layer on both sides by DC sputtering. The typical beam current was about 100 pA. In the second experiment our sample was a 1 mm thick glass plate, in which capillaries with diameter of 5 μm and length of 1 mm were arranged in a regular, dense pattern. This sample is a piece of a multichannel plate, provided by an MCP manufacturer without the coating layer for secondary electron emission. The geometric opening of the sample was 52 %. Like for the PC sample, both side of it was covered with gold. The used typical beam current was about 720 pA. We measured the integrated ion beam current on the front surface of the sample for normalization. Since it is measured at a surface (not in a Faraday cup), it also has a secondary electron component. Nevertheless, the measured current is rather accurately proportional with the net ion current, so it can be applied for normalization to avoid the intensity variations caused by the fluctuating incident beam. In order to calibrate for the real incident current, we measured the secondary emission rate by measuring the same current at the sample front and in a Faraday cup. The beam divergence and the size of the beam on the sample were estimated from the collimator size (0.5 mm) and from the spot diameter of an intensity reduced beam in the MCP surface. The sample holder is on half way between the collimator and the MCP. The typical beam divergence was $\pm 0.4^\circ$ in both experiments.

We measured two-dimensional transmission profiles for Ar ions at different tilt angles relative to ion beam, together with those for the transmitted neutrals [7]. In order to measure the time development of the guiding effect, we performed a long set of expositions. The time sequence consisted of 9 seconds data collection periods followed by 1 second breaks between the expositions. One of the collected MCP pictures of 9 seconds exposition time is seen in figure 2 for the glass capillaries. We observed only the Ar^{7+} ions and neutralized projectiles, i. e., Ar atoms. The spot for the ions is much larger than that for the neutrals. This observation shows that the angular spread of the transmitted ions are enlarged compared to that geometrically is expected. We note that intermediate charge states were not observed in

the present set of experiments, even when the angular spread of ions was smaller, allowing a better separation.

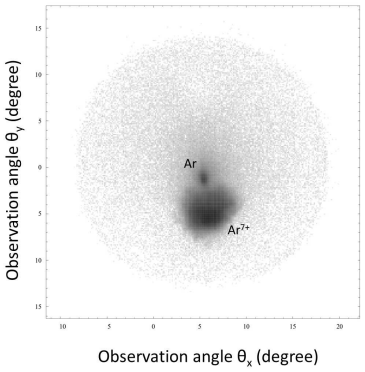

Figure 2: One of the collected MCP images at 5° tilt angle in the case of the glass sample after the the start of guided transmission. The difference between the Θ_y positions of the neutral Ar atoms and Ar^{7+} ions is caused by the electrostatic deflection field applied in front of the detector.

III. Results and discussion

The main goal in both experiments was to study the dynamic behavior of the transmission of ions and outgoing neutrals. For the PC capillaries, the development of the transmission in function of deposited charge is shown in Fig. 3. At a constant incoming current, the total charge, which is deposited to the sample is proportional with time. Both earlier experiments and model considerations show that, if the current is varied, the development of the guided transmission scales with the deposited charge. Therefore we exhibit our data as a function of deposited charge in the Figures. As it is clearly seen in figure 3(a), the ion-intensity started from zero as it was expected. After a short delay the transmitted intensity increased rapidly until reaching a maximum. Deducing from the regular cases for ion-guiding [1-6] the transmitted intensity of the Ar^{7+} ions is expected to stay around this maximum in an equilibrium state. The perpendicular component of the

developing electrostatic field deflects the ions. However, the electrostatic gradient has a parallel component too, which can decelerate the ions. This deceleration increases the beam divergence, so the ions can hit the wall easier, and can deposit their charge. Thus again increase the repulsive force for ions. When the field strength increases a non-linear pre-breakdown process develops at the surface, which takes away the excess charges no matter how large the incoming current is [2, 8]. A balance between this nonlinearly increasing depletion current and the current of charge deposition ensures the stability of the transmission in the equilibrium state, or, if the equilibrium field is too large, leads to the blocking effect.

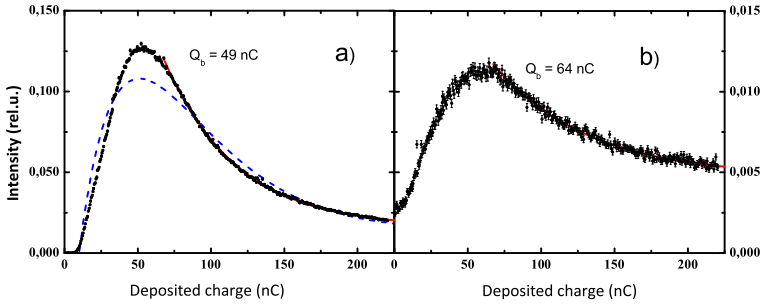

Figure 3: The transmitted intensity of Ar^{7+} ions (a), and Ar atoms (b) as function of deposited charge. Results are from ref. [8]. The capillaries were tilted by 5° with respect to the beam. The black points are experimental results with error bars. Dashed line represents a fit by a model function (Eq. 1) for ions (blue dashed line). The decreasing parts are well described by an exponential decay function (red solid lines). The characteristic values for blocking Q_b are indicated for both curves.

The starting region of guiding for the PC sample shows the common behavior for the majority of studied cases. Ions appear with a definite delay after the beam to hit the sample. In contast, neutral particles (Ar atoms) appear immediately with a finite yield. The reason is that the ions hit the capillary wall in the entrance region immediately, and some of the neutralized projectiles are scattered into the direction of the capillary exit. For ion transmission, however, a minimum amount of charge deposition is needed. Above this threshold value, the ion transmission starts to increase

rapidly. After arriving the maximum, however, our PC sample do not stay at an equilibrium transmission, the intensity starts to decrease. From Fig. 3, it is clearly seen that it falls down to relatively small value. For neutrals less dramatic decrease was observed in the intensity. The different behavior shown for Ar atoms and Ar^{7+} ions is originating from the fact that neutrals may originate from multiple sources. They can be created in the entrance region, where ions are impinging and neutralized at the capillary wall, to form the charged patch and they can also be created from the guided ions at the exit region. The latter mechanism results in similarities in the time evolution of ions and neutrals. The characteristic deposited charge value for blocking, Q_b was higher for larger tilt angles showing that blocking is faster for smaller tilting. To describe the raising and blocking part of the measured curves we use a phenomenological approach by this formula[8]:

$$f(Q_d)=\begin{cases} 0, & \text{if } Q_d < Q_s \\ f_0\left(1-e^{\left(-\frac{Q_d-Q_s}{Q_c}\right)}\right)\left(e^{\left(-\frac{Q_d-Q_s}{Q_b}\right)}+K\right), & \text{if } Q_d \geq Q_s \end{cases} \quad (1)$$

Here, Q_d is the deposited charge, Q_s is a threshold value introduced to describe the period until there is no transmission. The first term in brackets describes the rising part [8] with Q_c as a characteristic charge constant. The second term is for describing the blocking effect. This is an exponentially decaying function with characteristic charge Q_b. Since the intensities seem to approach a non-zero constant value at the end, an additive K constant was introduced in the blocking term, too. Within the nonlinear model outlined above, the blocking effect can be explained by supposing that the field strength at the wall is still far from the nonlinear pre-breakdown regime when a potential barrier which able to stop the ions develops in the capillaries. The development of blocking is accelerated by the defocusing of the beam of strongly decelerated ions during partial blocking. It can be considered as a kind of positive feedback. As a result, ion deposition is more and more concentrated to the entrance region of the capillaries, but never stops. Since ion deposition always produces some neutrals, which are not affected by electric fields any more, the intensity of the observed neutral atoms should decrease much slower than that of the ions, even if

the blocking effect is strong. This is in good agreement with the tendencies shown in Fig. 3. We note that a higher capillary density should result in a higher density of deposited charges in the middle region of the capillaries, leading to an even faster increase of the repulsive voltage in this region. Therefore, higher density may accelerate the development of the blocking significantly. Model calculations for confirming the above picture are in progress. In the case of the glass sample, as figure 4 shows, the time evolution of the transmission is very slow. The transmitted ion intensity remained under 0.6 percent after a few hours of irradiation. (see fig. 4 (b)). To accelerate the process we needed higher beam current, which lead to over exposure problems in counting. The observed behavior is similar to other samples: there is a threshold for non-zero transmission and after the intensity increases (see fig. 4(a)). The increase, however, is very slow.

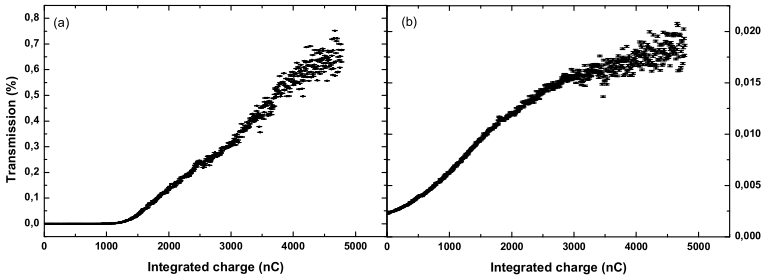

Figure 4: The transmitted intensity of Ar^{7+} ions (a), and Ar atoms (b) as function of deposited charge. The capillaries were tilted by 5° with respect to the beam. The points with error bars are experimental results.

The transmitted intensity did not reach the maximum, when the detector was already overloaded. This problem cannot be solved by decreasing the ion beam current, since the evolution of the guiding would become much slower. In order to record the full time development, we plan to repeat the experiment with higher beam current using other detection technique, which is able to record higher intensities, for example sensitive current measurement. We note that the development of guiding for a single borosilicate capillary with 4.5 keV Ar^{9+} impact at 150 pA [9] appeared to be much faster than that of our present sample. Therefore the present results may be explained by collective effects of the neighbouring capillaries in the high

density sample.

IV. Summary

In summary, blocking effect was observed for both the guided ions and for the neutrals with similar dynamic behavior in the case of PC foil. A borosilicate glass sample did not show the blocking effect, but its time evolution was very slow, probably due to the high density and aspect ratio of the capillaries.

Acknowledgement

This work was supported by the Hungarian National Science Foundation (OTKA, Grant No. K73703), and by the TÁMOP-4.2.2/B-10/1-2010-0024 project, which is co-financed by the European Union and the European Social Fund.

References

[1] N. Stolterfoht *et al*, Phys. Rev. Lett. **88**, 133201 (2002)

[2] N. Stolterfoht *et al*, Nucl. Instrum. Methods B **203**, 246 (2003)

[3] M. B. Sahana *et al*, Phys. Rev. A **73**, 040901(R) (2006)

[4] S. Mátáfi-Tempfli *et al*, Nanotechnology **17**, 3915 (2006)

[5] Y. Kanai *et al*, Phys. Rev. A **79**, 012711 (2009)

[6] K. Schiessl *et al*, Phys. Rev. A **72**, 062902 (2005)

[7] Z. Juhász *et al*, Nucl. Inst. Meth. B **279**, 177-181 (2012)

[8] N. Stolterfoht *et al*, Nucl. Inst. Meth. B **235**, 460 (2005)

[9] G. Kowarik *et al*, Nucl. Inst. Meth. B **267**, 2277 (2009)